Synthesis of artificial cells *via* biocatalytic polymerisation-induced self-assembly

Sètuhn Jimaja,[a‡] Andrea Belluati,[b,c‡*] Robert J. Chadwick,[b] Christopher Glynn,[b] Mohamed Chami[d], Dominic Happel[c], Chao Guo[b], Harald Kolmar[c], and Nico Bruns[b,c*]

[a]Adolphe Merkle Institute, University of Fribourg, Chemin des Verdiers 4, 1700 Fribourg, Switzerland.
[b]Department of Pure and Applied Chemistry, University of Strathclyde, Thomas Graham Building, 295 Cathedral Street, Glasgow G1 1XL, United Kingdom.
[c]Department of Chemistry and Centre for Synthetic Biology, Technical University of Darmstadt, Peter-Grünberg-Straße 4, 64287 Darmstadt, Germany.
[d]Biozentrum, University of Basel, Spitalstrasse 41, 4056 Basel, Switzerland.

‡Authors contributed equally to this work

*andrea.belluati@tu-darmstadt.de, nico.bruns@tu-darmstadt.de

Supporting Information

MATERIALS

Compounds

Polyethylene glycol monomethyl ether (mPEG, 5 kDa), bromoisobutyryl bromide, triethylamine (Et_3N), sodium ascorbate (NaAsc), myoglobin (Mb), hydroxypropyl methacrylate (HPMA), Tris-HCl, dimethylformamide (DMF), 4-(dimethylamino)pyridine (≥98%, DMAP), RPMi-1640 (with addition of fetal bovine serum (10%), L-glutamine (1%), penicillin-streptomycin (1%)), FITC-dextran 40kDa, β-galactosidase (β-Gal), glucose oxidase (GOX), alkaline phosphatase (ALP), actin, Atto488 NHS-ester, phalloidin Atto565, calcium glycerophosphate (CaGP), fluorescein di(β-D-galactopyranoside) (FDG), fluorescein diacetate (FDA), and propidium iodide (PI) were purchased from Sigma-Aldrich and used as received. Tetrahydrofurane (THF) and dichloromethane (CH_2Cl_2) were purchased from Acros Organics. *E. coli* T7 S30 Extract System for Circular DNA was purchased from Promega. All solvents were purchased in high purity. All reactions requiring anhydrous conditions were carried out using dried Schlenk glassware and under inert Ar gas atmosphere. Deuterated solvents were purchased from Cambridge Isotope Laboratories. PBS 10X was prepared and NaBr was added to make PBS-Br 1X (NaBr 100 mM). Alexa405 SiO_2 NPs were a gift by Prof. Alke Petri-Fink (Adolphe Merkle Institute, University of Fribourg, Switzerland).[1]

Plasmids

pNCS-mClover3 was a gift from Prof. Markus Biesalski (TU Darmstadt).[2] ZP9 Actin was a gift from Randall Moon (Addgene plasmid # 16932; http://n2t.net/addgene:16932; RRID:Addgene_16932), Chx10 3kb AP (CC#318) was a gift from Connie Cepko (Addgene plasmid # 15205; http://n2t.net/addgene:15205; RRID:Addgene_15205).[3] pNCS-mClover3 was propagated in *E. coli* BL21 (DE3), whereas ZP9A and CHx10 3kbAP were propagated in *E. coli* DH5alpha. All cultures were grown in Luria-Bertani broth supplemented with the antibiotic they would be resistant to (ampicillin or kanamycin) until OD_{600} 1. Then, the plasmids were purified using a QIAprep Spin Miniprep Kit (Qiagen, USA). The amount of purified DNA was quantified at 260 nm using a NanoDrop One/One^C UV-Vis Spectrophotometer (Thermo Scientific).

EXPERIMENTAL PROCEDURES

SYNTHESIS OF POLY(ETHYLENE GLYCOL) METHYL ETHER 2-BROMOISOBUTYRATE (MPEG-BIB)

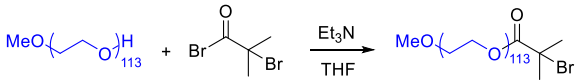

Scheme 1. Synthesis of mPEG-BiB.

mPEG-BiB was synthesised according to a literature procedure.[4] Briefly, mPEG (5000 g mol^{-1}, 2.5 mmol) was dissolved in dry THF (100 mL) under an argon atmosphere and the solution was cooled on ice. Then, triethylamine (0.37 mL, 2.7 mmol, 1.1 eq) was added, followed by 2-bromoisobutyrylbromide (0.33 mL, 2.7 mmol, 1.1 eq). After overnight stirring, the product was filtered. The filtrate was concentrated at reduced pressure and the residue was redissolved in dichloromethane. The product was then isolated by precipitation with diethylether and then dried under vacuum.

BIOPISA

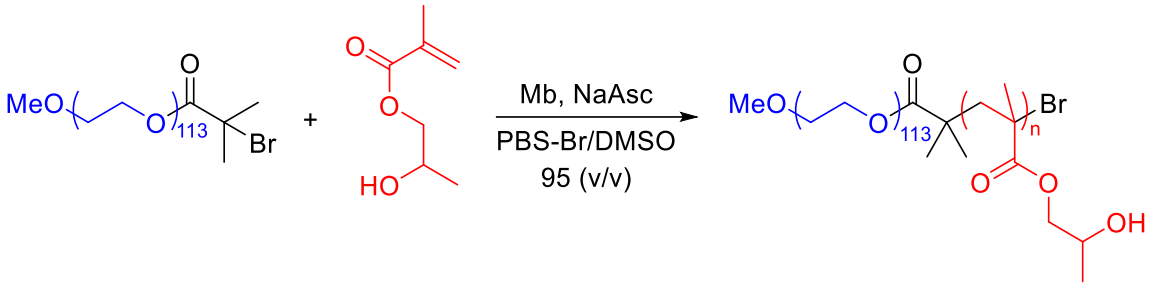

Scheme 2. Typical bioPISA reaction.

In a typical bioPISA experiment, HPMA (2 mL, filtered on basic alumina) was measured in a 4 mL vial that was closed with a septum. A certain amount of mPEG-BiB and sodium ascorbate was dissolved in a certain volume PBS-Br buffer pH 7.4 spiked with 5 vol% DMSO in a 4 mL vial closed with a septum. A certain amount of myoglobin was suspended in PBS-Br buffer pH 7.4 in a 10 mL Schlenk flask. All the solutions were degassed with Ar for 1 h. The mPEG-BiB/NaAsc solution was added to the Schlenk flask, and the resulting solution was stirred for 15 min. The colour of the reaction mixture changed from brown to red (myoglobin oxidation). Then, purified HPMA was added. The reaction mixture was stirred for 4 h at room temperature before being opened to air to quench the polymerization by atmospheric oxygen. The final suspension was diluted with 15 mL of PBS. The reagent amounts are specified in **Table S1**. All encapsulations were performed with HPMA 25 wt% and aimed DP 400.

TECHNIQUES

NMR SPECTROSCOPY

NMR spectra were recorded on a Bruker Avance III 300 MHz NMR spectrometer (^{1}H NMR 300 MHz) or a Bruker Avance III 400 MHz NMR spectrometer (^{1}H NMR 400 MHz) using deuterated dimethyl sulfoxide (DMSO-d_6) as the solvent. Chemical shifts of protons are reported as δ in parts per million (ppm) and are relative to DMSO-d_6 at δ = 2.54 ppm. Data were evaluated with the MestReNova software suite (v 12.0).

SIZE EXCLUSION CHROMATOGRAPHY

To analyse the resulting block copolymers by size exclusion chromatography (SEC), the DP 350, 20 wt% reaction mixtures was centrifuged, and the supernatant removed. The precipitate was diluted in THF. Copolymer samples were prepared as follow: the bioPISA suspension was centrifuged (13000 rpm) and the supernatant was removed. The sample was resuspended in 18 mL DI water, and the purification was repeated 4 times. The remaining residue was let to dry overnight at 40 °C and then suspended in 2 mL THF. The supernatant was passed through a 0.2 µm syringe filter (Whatman® Puradisc 13, PP) before analysis by THF SEC.

SEC experiments were performed on an Agilent 1200 series HPLC system equipped with an Agilent PLgel mixed guard column (particle size= 5 µm) and two Agilent PLgel mixed-D columns (ID = 7.5 mm, L = 300 mm, particle size = 5 µm). Signals were recorded by a UV detector (Agilent 1200 series), an Optilab REX interferometric refractometer, and a miniDawn TREOS light scattering detector (Wyatt Technology Corp.). Samples were run using THF as the eluent at 30 °C and a flow rate of 1.0 mL min^{-1}. Data analyses were carried out on Astra software (Wyatt Technology Corp.) and molecular weights were determined based on narrow molecular weight polystyrene standards calibration (from 540 to 2'210'000 g mol^{-1}).

DYNAMIC LIGHT SCATTERING (DLS)

One drop of the suspension was diluted in deionised water (2 mL). DLS measurements of PISA assemblies were performed on a Zetasizer Nano ZSP (Malvern Instruments, UK) at 25 °C, 173°. Stock solutions were diluted 1:1000 in PBS in a cuvette, with a final volume of 1 mL, measured during 11 runs, repeated three times. Alexa 405-tagged SiO_2 NPs were instead measured according to the same protocol, on a Zetasizer Nano ZS90, at 25°C and 90°. Because of the large size of the polymersomes, only the smaller spherical morphologies were analysed by DLS.

REACTION KINETICS

BioPISA reactions were prepared as described and DMSO was replaced by DMF to allow monitoring of the monomer concentration by NMR spectroscopy. Reaction mixtures samples (0.1 mL) were taken at t = 0 and every 10 min and diluted in DMSO-d_6 (0.5 mL) before analysis by ^{1}H NMR spectroscopy.

CONFOCAL LASER SCANNING MICROSCOPY (CLSM)

Imaging of vesicles was performed on a Leica SP8 CLSM, equipped with an HCX PL APO 63 × NA 1.2 W CORR CS2 objective (Alexa 405: ex. 405 nm, em. 410 – 430 nm; Fluorescein, mClover, FITC, Atto488: ex. 488 nm, em. 505 – 525 nm; Resorufin, Atto565: ex. 561 nm, em. 570 – 590 nm; Cy5, PI: ex. 635 nm, em. 660 – 690 nm). Membranes were stained with Cy5-$PEG_{3.5k}$-cholesterol, synthesized according to a published procedure.[5] Images were optimized (brightness and contrast; applied evenly throughout a whole image) and analysed via ImageJ. Z-stacks were processed using LAS X software (Leica Camera AG, Germany).

ENCAPSULATION EFFICIENCY

Several cargoes were co-encapsulated together with Mb. Depending on the sample, we added to the reaction mixture:

- 32 µL FITC-dextran 40kDa 10 mg ml^{-1}
- 10 µL B-gal 10 mg ml^{-1}
- 10 µL Alexa405 SiO_2 NP 1% w/v%

To quantify the encapsulation efficiency, post-polymerization aliquots were diluted 1:10 in PBS, and run through PD 10 desalting columns (Cytvia; gravity protocol) to remove the unencapsulated molecules. The second fraction

(7 mL, per supplier's instructions) was recovered as well. Alexa405 SiO_2 NP were instead recovered by centrifuging a 1 mL-aliquot of vesicles (500 x g, 3 min, in an Eppendorf microcentrifuge), and recovering the supernatant.

For FITC-dextran and Alexa405 SiO_2 NP, a calibration curve was used to quantify the encapsulated fluorophores in the second fraction, on a Clariostar Plus plate reader (BMG Labtech, Germany), in a Greiner transparent 96-well plate.

In the case of Mb, the absorbance at 280 nm in the second fraction was quantified, with ε = 13.98 mM^{-1} cm^{-1}, from its sequence, as of (N of tryptophan residues*5.5) + (N of tyrosine residues*1.5).[6] For β-gal, the protein absorbance at 280 nm was likewise calculated, using the expected content of Mb as blank, with ε= 191.95 mM^{-1} cm^{-1}. The measurements were conducted in a Cary 60 UV-Vis spectrophotometer (Agilent, USA).

FITC-labelled polystyrene microbeads (2 µm diameter) were added to the reaction mixture (10 µL directly from the suspension) and then directly imaged via CLSM.

To quantify unencapsulated Mb after washing of the 1st fraction, the absorbance values after bicinchoninic acid assay (Merck Millipore, protocol according to manufacturer's manual) were compared in GUVs, GUVs after centrifugation (500 x g, 3 min, in an Eppendorf microcentrifuge, 2x) and washing with PBS, and the resulting washing supernatant. Volumes of both GUVs and supernatant were kept constant.

CO-ENCAPSULATION OF GLUCOSE OXIDASE (GOX)

To obtain GOX-loaded vesicles, GOX was dissolved (1 mg mL^{-1}) together with Mb in the reaction mixture. Then, the vesicles were purified. If needed, samples were incubated 10 minutes in a 1 mg mL^{-1} NaAsc solution before being centrifuged and resuspended (2x) in PBS again.

ENZYME ACTIVITY OF MB

The enzymatic activity of Mb was measured in a Clariostar Plus plate reader, in a Greiner transparent 96-well plate. In each well, 10 µL of vesicles (with Mb alone, or with GOX co-encapsulated) were mixed with 2 µL Ampliflu Red (also known as Amplex Red, AR) 100 µM, 5 µL H_2O_2 0.01%, to a final volume of 200 µL of PBS or PBS + 20 mg mL^{-1} glucose (with GOX present), and the fluorescence at 570/595 nm (±10 nm) was recorded, between 10 and 60 minutes.

ENZYME ACTIVITY OF B-GALACTOSIDASE (B-GAL)

To obtain β-gal-loaded vesicles, 100 µL of a 10 mg mL^{-1} enzyme solution was added to the reaction mixture. The enzymatic activity of β-gal was measured in a Clariostar Plus plate reader, in a Greiner transparent 96-well plate. In each well, 10 µL of vesicles encapsulating β-gal were mixed with 10 µL fluorescein Di-β-D-galactopyranoside (FDG), the formation of fluorescein was followed at 495/535 (±10) nm.

ENZYME ACTIVITY OF ALKALINE PHOSPHATASE (ALP)

To obtain ALP-loaded vesicles, 10 µL of alkaline phosphatase (13 mg ml^{-1}) were added to the reaction mixture. Once purified, the enzymatic activity of β-gal was measured in a Clariostar Plus plate reader. 10 µL of vesicles were mixed with 2 µL *para*-nitrophenylphosphate (pNPP) 1 mM, to a final volume of 200 µL in Tris-HCl. The formation of para-nitrophenol was followed at absorbance 405 nm.

The first fraction was subjected to several centrifugation and washing steps. All resulting supernatants and GUVs were incubated with trypsin (final concentration 0.5 mg mL^{-1} into 100 µL of sample) for 2 hours at 37 °C, and the resulting activities were compared to non-trypsinized samples. Volumes of both GUVs and supernatant were kept constant. The values were analysed with a t-test.

ACTIN POLYMERIZATION

Actin was labelled with Atto 488-NHS ester, by reacting 1 mg of protein in 1 mL PBS, with 1 mM dye, 37 °C, 1 h, and then purifying the mixture with a 10 kDa spin diafiltration device (Amicon, Merck). 100 µL of actin 1 mg mL^{-1} and 10 µL of Actin-Atto 488 were added to the Mb mixture. The solvent used was Tris-HCl, pH 7.5, with the addition of 100 mM NaBr. After purification, the vesicles were imaged by diluting them either in Tris-HCl, or $MgCl_2$ 100 mM.

CALCIUM PHOSPHATE BIOMINERALIZATION

10 µL of alkaline phosphatase (ALP, 13 mg ml^{-1}) were added to the reaction mixture. In an Eppendorf tube, 100 µL of the purified sample were mixed with 50 µL calcium glycerophosphate 100 mM and 5 µL fluorescein 10 mM, then incubated at 37 °C, 4 h. The cleaving of glycerophosphate (CaGP) by ALP was confirmed visually by the formation of a white precipitate. The samples were then imaged via CLSM.

POLYMERIZATION IN PRESENCE OF BACTERIA

100 µL of *E. coli* BL21 (DE3) expressing mClover at OD_{600} 1 were added to the reaction mixture. After the polymerization, the monomer conversion yield was measured via NMR spectroscopy. To image the structures, the polymer membranes were stained with Cy5-$PEG_{3.5k}$-cholesterol. For viability measurements post polymerization, non-fluorescent *E. coli* were incubated with a final 0.5 mM of fluorescein diacetate; 1 µM propidium Iodide (PI) was selected as a stain for dead cells, and substituted Cy5-$PEG_{3.5k}$-cholesterol. 100 cells per conditions were imaged (either green or red fluorescent). Bacteria incubated at 95 °C for 10 minutes were the negative control.

PLASMID ENCAPSULATION AND CELL-FREE EXPRESSION

The cell-free expression of proteins within GUVs was achieved using the Promega *E. coli* S30 Extract System for Circular DNA (L1020). 75 µl of plasmid, at different concentrations (pNCS-mClover3: 300 ng mL^{-1}; ZP9A Actin: 98.4 ng ml^{-1}; Chx10 3kb AP: 137 ng ml^{-1}), 50 µL of S30 EXTRACT (cell lysate) were added to the reaction mixture. For ZP9A Actin, 10 µL of Phalloidin Atto565 (20 µM in MeOH) were added as well. After polymerization, to 70 µL of sample, 50 µl of S30 premix (containing the energy regenerating system) and 10 µL of complete amino acid mixture were added. The sample was incubated at 37 °C for 3 h, either split in 3 wells per condition (mClover synthesis) or in Eppendorf tubes. Afterwards, they were imaged via CLSM. Actin-containing vesicles were resuspended in 100 mM $MgCl_2$, whereas ALP-containing ones were first incubated in CaGP according to the protocol described above.

FLOW CYTOMETRY

For cytometric analysis of vesicles, the CytoFLEX S by Beckman Coulter was used (CytExpert Version 2.4.0.28). Samples were diluted prior to measurement with PBS to achieve an abort rate below 10%. To account for small particle size compared to cells, the primary threshold (trigger level) and the width channel were set to SSC (height: 1000). 50000 events per sample were recorded and a gating strategy was applied to exclude debris (SSC-A [log] vs FSC-A [log]) and to analyse only single vesicles per event (SSC-A [log] vs SSC-Width [linear]). Fluorescence of mClover was measured in the FITC channel (525/40 nm) at maximum gain due to small particle size.

TRANSMISSION ELECTRONIC MICROSCOPY

Dry-state-stained transmission electron microscopy (TEM) imaging was performed on Tecnai Spirit transmission electron microscope (TEM, FEI/ThermoFisher, Hillsboro, Oregon, United States) operating at 120 kV using a 2k Veleta camera (Olympus, Shinjuku, Tokyo, Japan). All dry-state samples were diluted with deionized water to appropriate analysis concentration and then deposited onto GO-coated copper grids. After roughly 1 min, excess

sample was blotted from the grid and the grid was stained with methylamine vanadate (Nanovan) negative stain solution for 1 min prior to blotting, drying and microscopic analysis.

CRYO-TRANSMISSION ELECTRONIC MICROSCOPY

A 4 µl aliquot of sample was adsorbed onto holey carbon-coated grid (Lacey, Tedpella, USA), blotted with Whatman 1 filter paper and vitrified into liquid ethane at -180 °C using a Leica GP2 plunger (Leica microsystems, Austria). Frozen grids were transferred onto a Talos Electron microscope (FEI, USA) using a Gatan 626 cryo-holder (GATAN, USA). Electron micrographs were recorded at an accelerating voltage of 200 kV using a low-dose system (40 e- $Å^{-2}$) and keeping the sample at -175 °C. Defocus values were -2 to 3 µm. Micrographs were recorded on 4K x 4K Ceta CMOS camera.

SUPPORTING INFORMATION

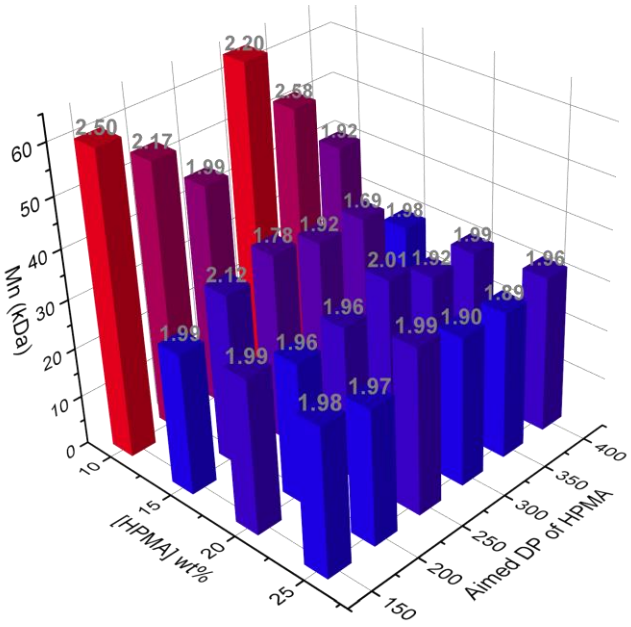

Figure S1. Molecular weight and *Đ* determined by SEC (THF, 30 °C, PS standard) of the resulting copolymer depending on the initial [HPMA] and aimed DP for bioPISA in PBS-Br. Note: as the molecular weight were around 30 kDa for [HPMA] > 10wt%, this suggests that the aimed DP is not the real DP and the important parameter could be the initiator concentration as was demonstrated for RAFT by Khor *et al*.[7]

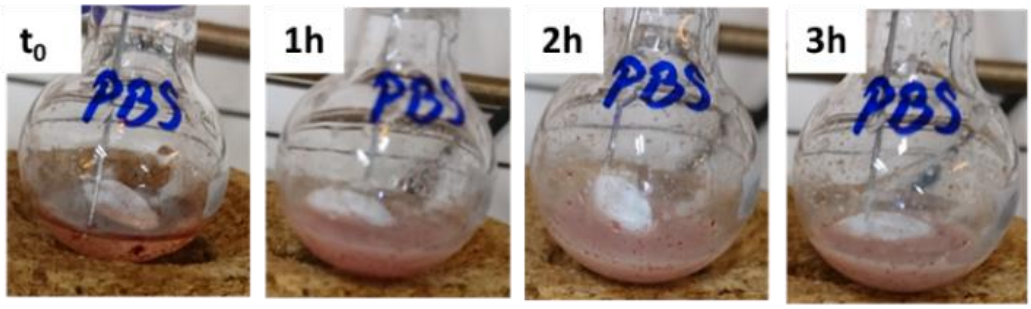

Figure S2. Photos of a bioPISA reaction mixture (**DP 150 10 wt%**) taken over time. The progressive increase in turbidity is due to the formation of nanostructures.

REACTION CONDITIONS

In control reactions, no reaction occurred without monomer, whereas reactions in which either mPEG-BiB, NaAsc, or Mb were omitted proceeded with a low monomer consumption of <20%. Thus, a low level of blank reaction happened, but the initiator, oxidising agent, and the metallo-protein are necessary for the reaction to proceed to high conversions (**Table S1**). The organic co-solvent DMF was necessary as well, likely as stabilizer for the growing chains.[8,9] Furthermore, polymerisations were unsuccessful when they were carried out in pure PBS or in a 100 mM NaBr solution in deionised water, indicating that both the salts in the PBS buffer and the NaBr were required for the polymerisation to happen, most likely because the buffer maintained the pH and NaBr maintained an excess of halides that is need for efficient ATRP in aqueous conditions.[10]

Table S1. Details of the bioPISA reactions conditions

EXPERIMENTS		CONDITIONS					
[HPMA] (wt%)	**Aimed HPMA (DP)**	**mPEG-Bib (mg)**	**Mb (mg)**	**HPMA (µL)**	**NaAsc (mg)**	**DMSO (mL)**	**PBS (mL)**
10	150	46 (1 eq)	4.7 (0.03 eq)	187 (150 eq)	11.9 (6 eq)	0.10	1.70
10	200	35 (1 eq)	3.6 (0.03 eq)	187 (200 eq)	8.3 (6 eq)	0.10	1.70
10	250	30 (1 eq)	3.1 (0.03 eq)	187 (250 eq)	7.4 (6 eq)	0.10	1.70
10	300	25 (1 eq)	2.6 (0.03 eq)	187 (300 eq)	5.9 (6 eq)	0.10	1.70
10	350	20 (1 eq)	2.0 (0.03 eq)	187 (350 eq)	4.8 (6 eq)	0.10	1.70
10	400	17 (1 eq)	1.7 (0.03 eq)	187 (400 eq)	4.0 (6 eq)	0.10	1.70
15	150	73 (1 eq)	7.4 (0.03 eq)	296 (150 eq)	17.6 (6 eq)	0.10	1.70
15	200	55 (1 eq)	5.6 (0.03 eq)	296 (200 eq)	13.1 (6 eq)	0.10	1.70
15	250	44 (1 eq)	4.5 (0.03 eq)	296 (250 eq)	10.5 (6 eq)	0.10	1.70
15	300	29 (1 eq)	3.8 (0.03 eq)	296 (300 eq)	12.0 (6 eq)	0.10	1.70
15	350	31 (1 eq)	3.2 (0.03 eq)	296 (350 eq)	7.4 (6 eq)	0.10	1.70
15	400	27 (1 eq)	2.8 (0.03 eq)	296 (400 eq)	6.4 (6 eq)	0.10	1.70
20	150	102 (1 eq)	10.4 (0.03 eq)	414 (150 eq)	24.3 (6 eq)	0.10	1.70
20	200	77 (1 eq)	7.9 (0.03 eq)	414 (200 eq)	18.3 (6 eq)	0.10	1.70
20	250	61 (1 eq)	6.2 (0.03 eq)	414 (250 eq)	14.5 (6 eq)	0.10	1.70
20	300	51 (1 eq)	5.1 (0.03 eq)	414 (300 eq)	12.1 (6 eq)	0.10	1.70
20	350	44 (1 eq)	4.5 (0.03 eq)	414 (350 eq)	10.5 (6 eq)	0.10	1.70
20	400	39 (1 eq)	4.0 (0.03 eq)	414 (400 eq)	9.3 (6 eq)	0.10	1.70
25	150	136 (1 eq)	13.9 (0.03 eq)	552 (150 eq)	32.3 (6 eq)	0.10	1.70
25	200	102 (1 eq)	10.4 (0.03 eq)	552 (200 eq)	24.3 (6 eq)	0.10	1.70
25	250	82 (1 eq)	8.4 (0.03 eq)	552 (250 eq)	19.5 (6 eq)	0.10	1.70
25	300	68 (1 eq)	6.5 (0.03 eq)	552 (300 eq)	16.2 (6 eq)	0.10	1.70
25	350	58 (1 eq)	5.9 (0.03 eq)	552 (350 eq)	13.8 (6 eq)	0.10	1.70
25	400	51 (1 eq)	5.2 (0.03 eq)	552 (400 eq)	12.1 (6 eq)	0.10	1.70

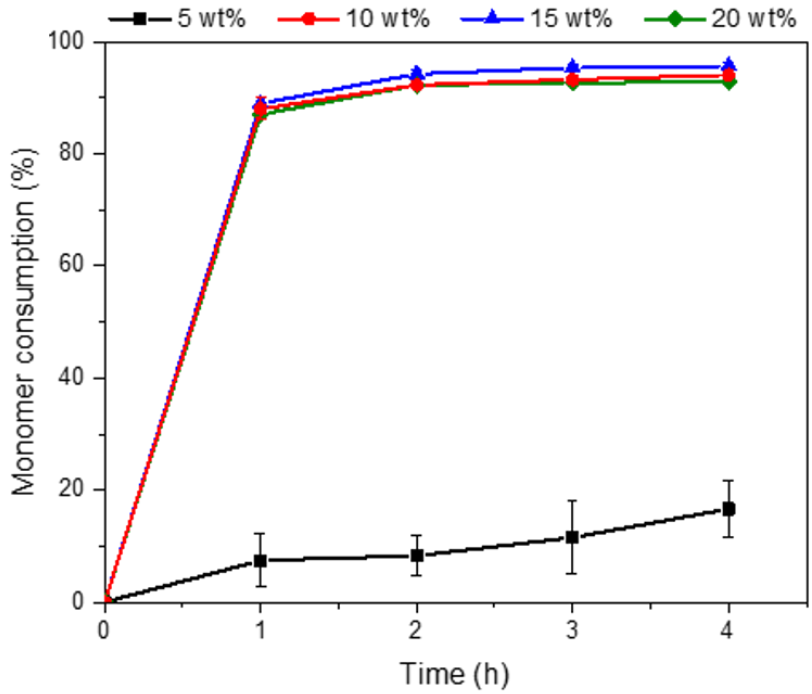

Figure S3. Monomer consumption over time ([HPMA] = 20 wt% and aimed DP = 150) at different initial monomer concentrations: 5 (black squares), 10 (red circles), 15 (blue triangles) and 20 (green diamonds) wt% with a HPMA aimed DP of 150. Error bars as mean ± SD, n = 3.

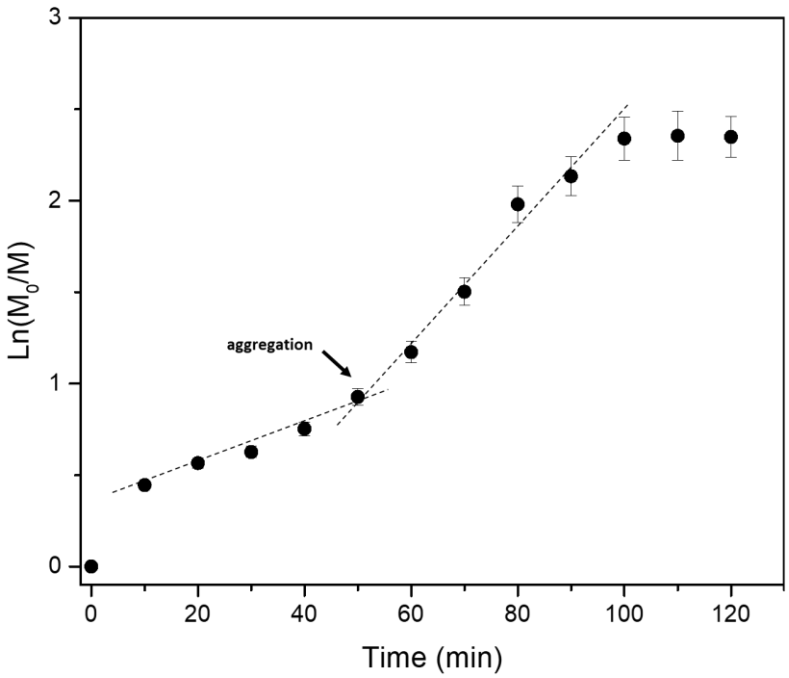

Figure S4. Kinetic data of bioPISA (DP 300 20 wt%) with 10 min intervals showing the onset of aggregation after 50 min of reaction before reaching a plateau at 100 min . Error bars as mean ± SD, n = 3.

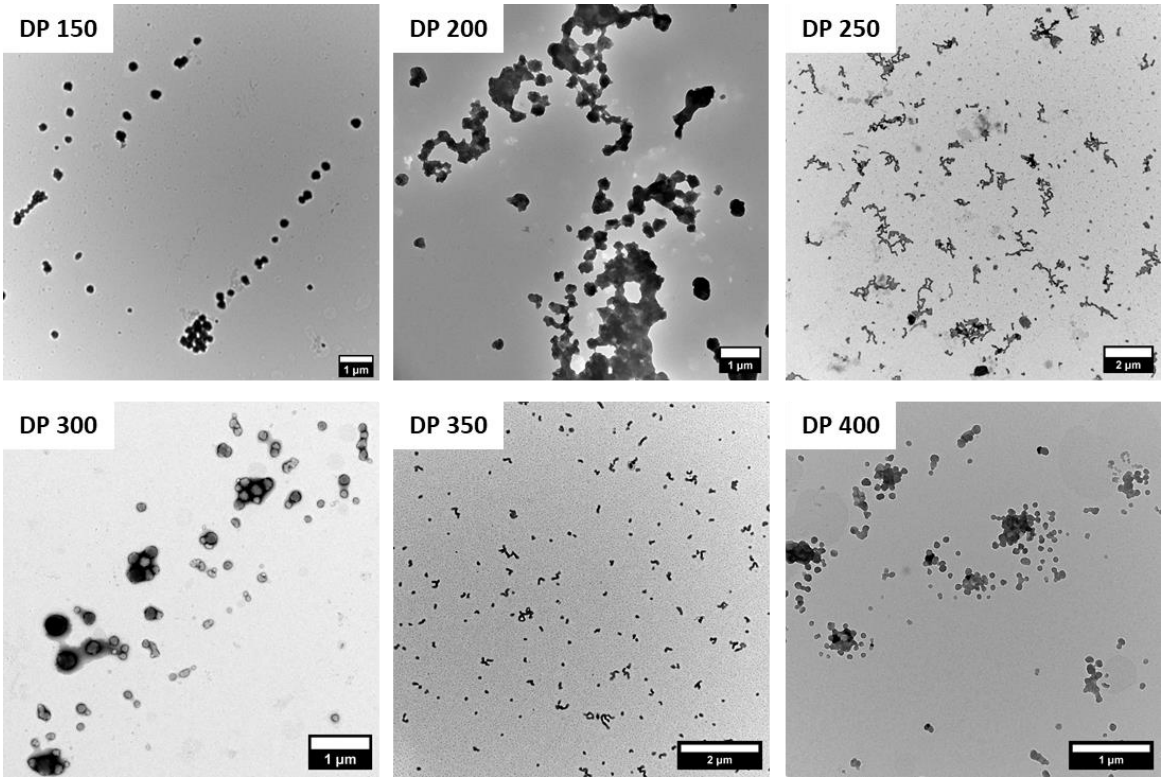

Figure S5. TEM images of morphologies from bioPISA at [HPMA] = 10 wt% and aimed DP = 150, 200, 250, 300, 350 and 400.

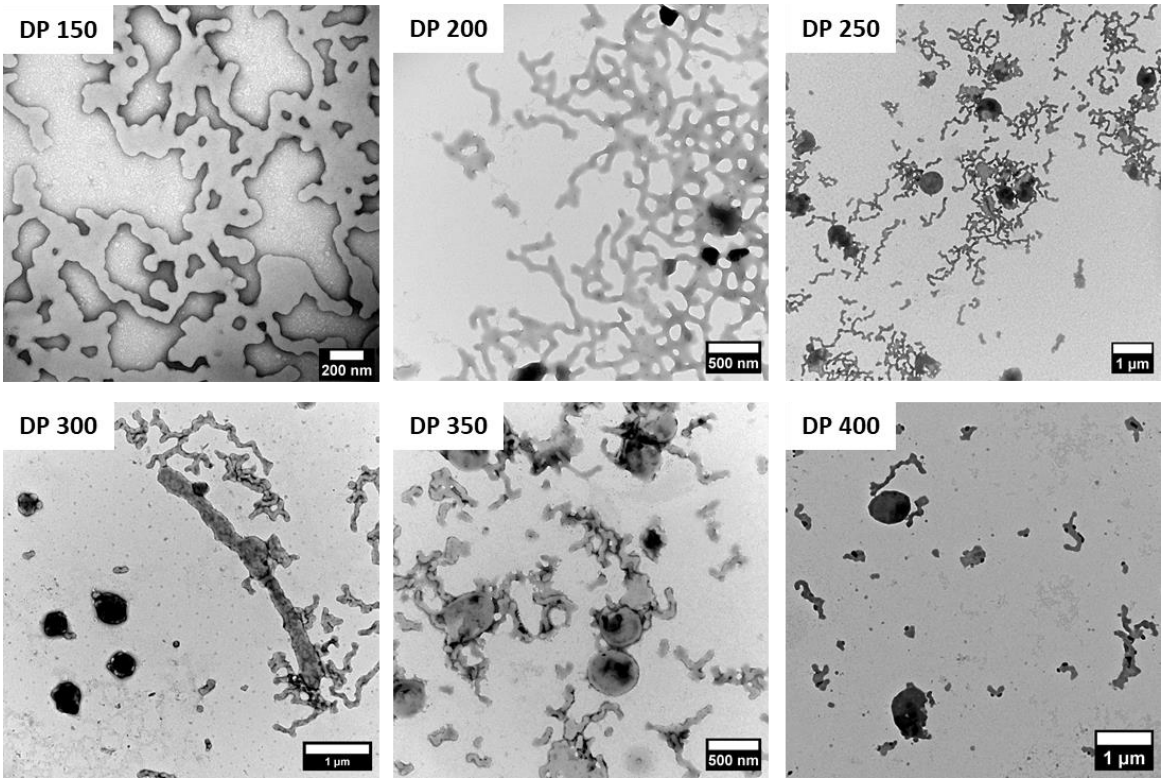

Figure S6. TEM images of morphologies from bioPISA at [HPMA] = 15 wt% and aimed DP = 150, 200, 250, 300, 350 and 400.

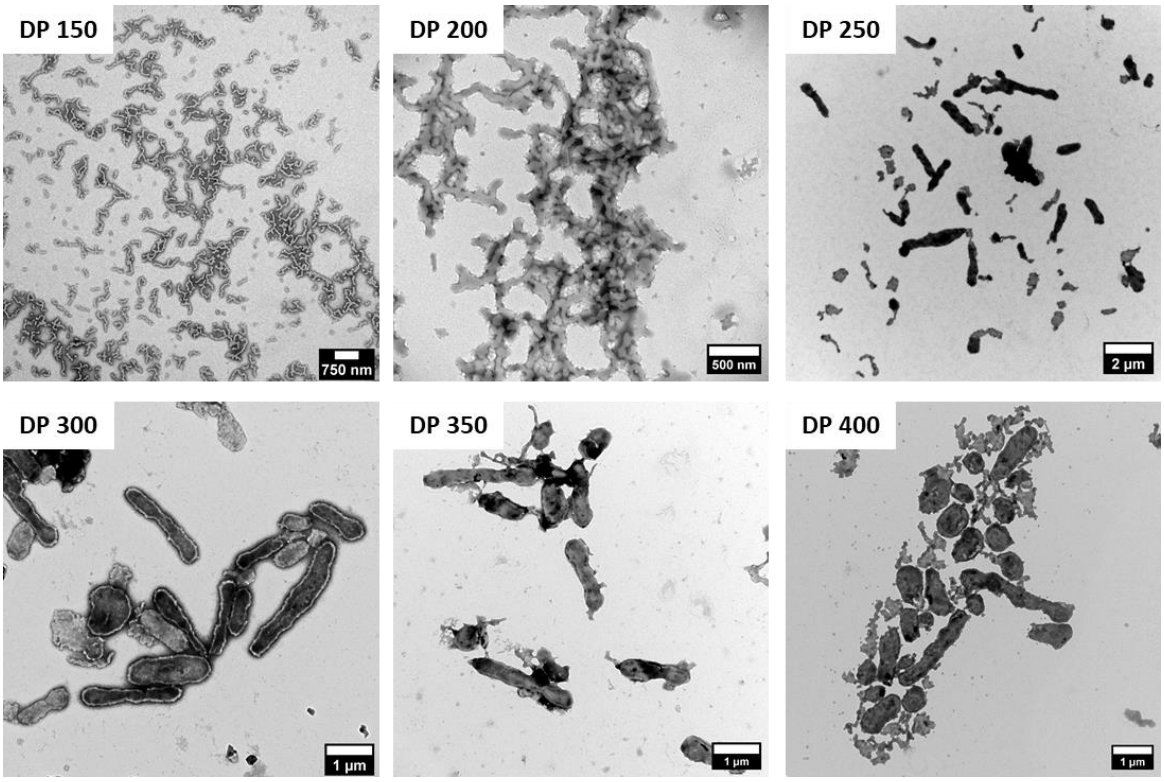

Figure S7. TEM images of morphologies from bioPISA at [HPMA] = 20 wt% and aimed DP = 150, 200, 250, 300, 350 and 400.

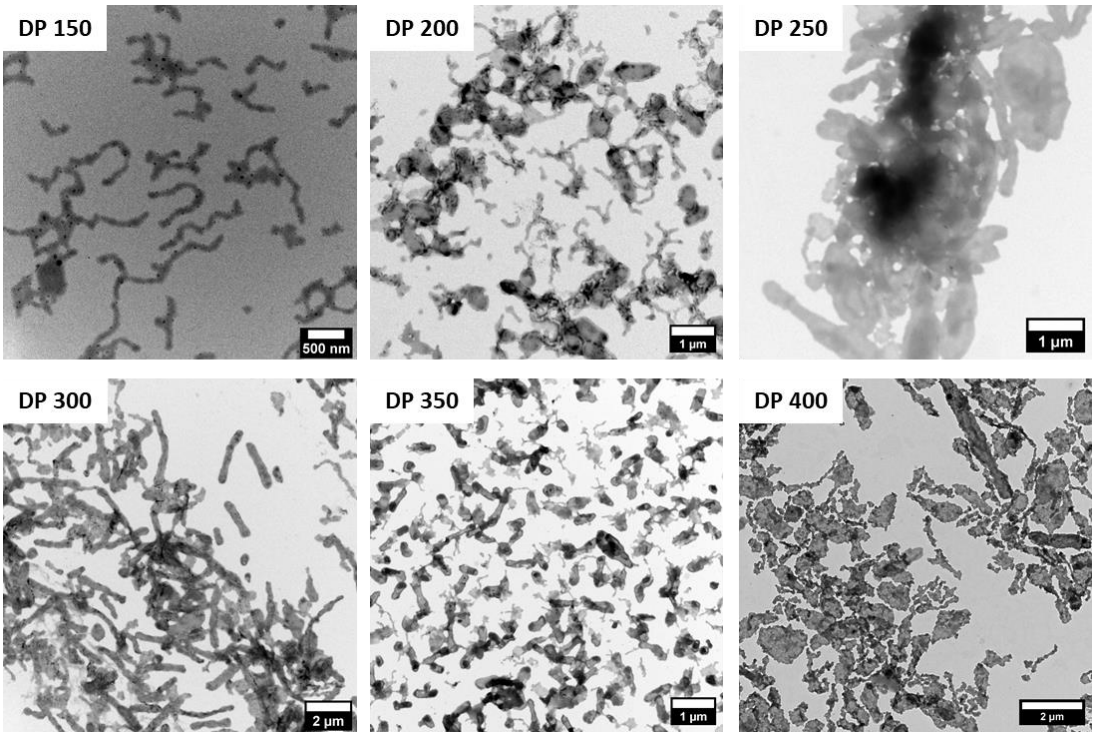

Figure S8. TEM images of morphologies from bioPISA at [HPMA] = 25 wt% and aimed DP = 150, 200, 250, 300, 350 and 400.

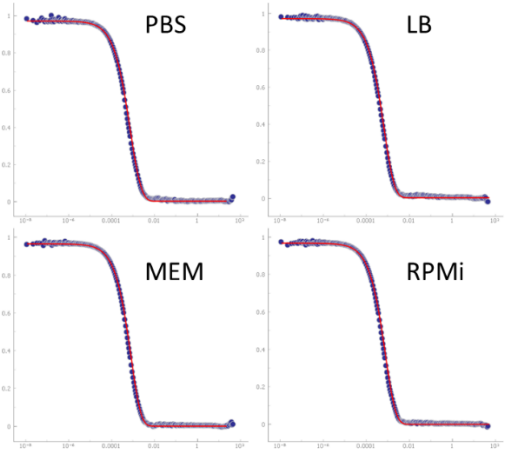

Solvent	D_h (nm)	PDI
PBS	238 ±22	0.28
LB	242 ±30	0.15
MEM	234 ±23	0.12
RPMi	208 ±24	0.12

[a] DLS 90 ° @ 25 °C, 10 × 60 s measurements. Cumular

Figure S9. DLS analysis (correlograms and numerical values) of the spherical nanostructures synthesised by bioPISA in PBS-Br at [HPMA] 10 wt% and aimed DP 150.

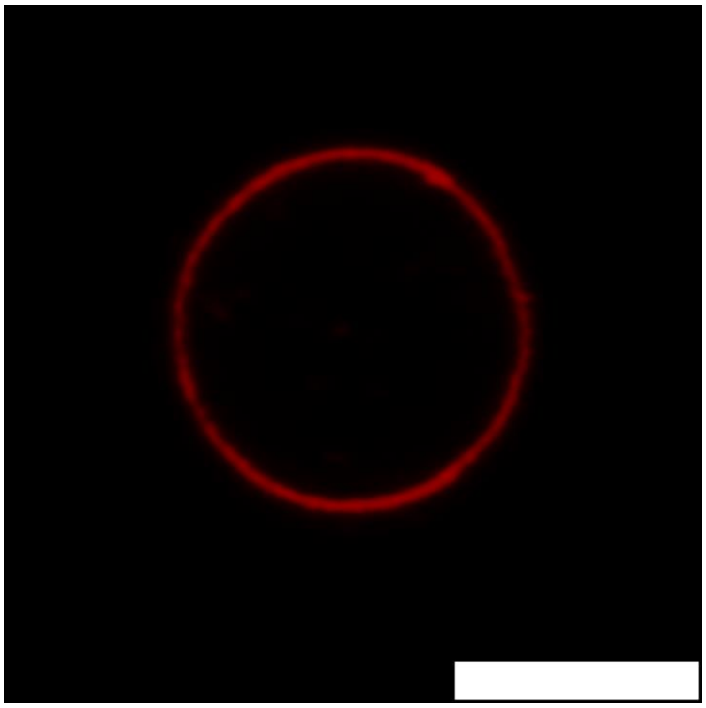

Figure S10. CLSM micrograph of a GUV obtained from bioPISA (red: Cy5-$PEG_{3.5k}$-cholesterol). Scalebar: **5 µm.**

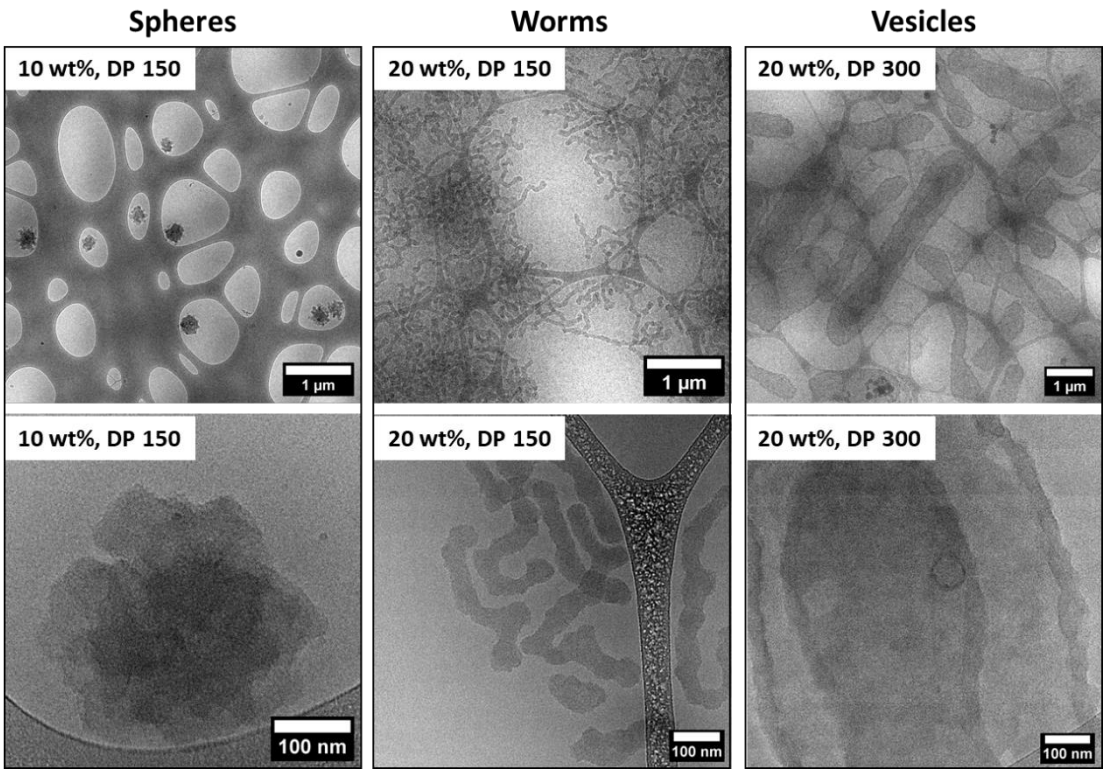

Figure S11. Cryo-TEM images of the three morphologies obtained by bioPISA in PBS-Br at [HPMA] = 10 wt% and aimed DP = 150 for the spheres, [HPMA] = 20 wt% and aimed DP = 150 for the worms and [HPMA] = 20 wt% and aimed DP = 300 for the vesicles.

SIZE EXCLUSION CHROMATOGRAPHY

The polymer was only partially soluble in the organic solvent. Several other solvents (DMF, DMSO, CH_2Cl_2, $CHCl_3$) were employed, but none achieved complete dissolution of the copolymer precipitate. It is hypothesised that cross-linking happened during the chain-extension, possibly due to transesterification of the side chains once inaccessible to the catalyst, which rendered part of the final copolymer insoluble.[11,12] The fraction of insoluble copolymer was 62% ± 8% irrespective of the molecular weight of the formed polymers or the morphology of the self-assemblies. The soluble parts of the bioPISA-derived diblock copolymers had number average molecular weights (M_n) of 30-60 kDa and dispersities ($Đ$) of 1.5-2.5 (**Figure S12** and **Table S1**). One explanation for the broad molecular weight distributions is that, unlike bioRAFT where the polymer chain does not need proximity to the enzyme to grow, ATRP necessitates the catalyst for the atom transfer (in this case Mb) to be close to the active polymer chain-end.[13] In PISA, the growing chain-ends are located in the hydrophobic core or membrane of the self-assemblies, and therefore difficult for the water-soluble enzyme to reach. This most likely led to a reduction in the degree of control of the polymerization and, as a result, in high dispersities. Thus, most likely the reaction proceeded through an ATRP-like initiation and initial RDRP until the block copolymers become water-insoluble, followed by a free radical polymerisation inside of the hydrophobic parts of the formed self-assemblies. While this might seem to be a disadvantage, it did not significantly affect the predictability of our method in generating a variety of self-assembled nanostructures, as discussed above.

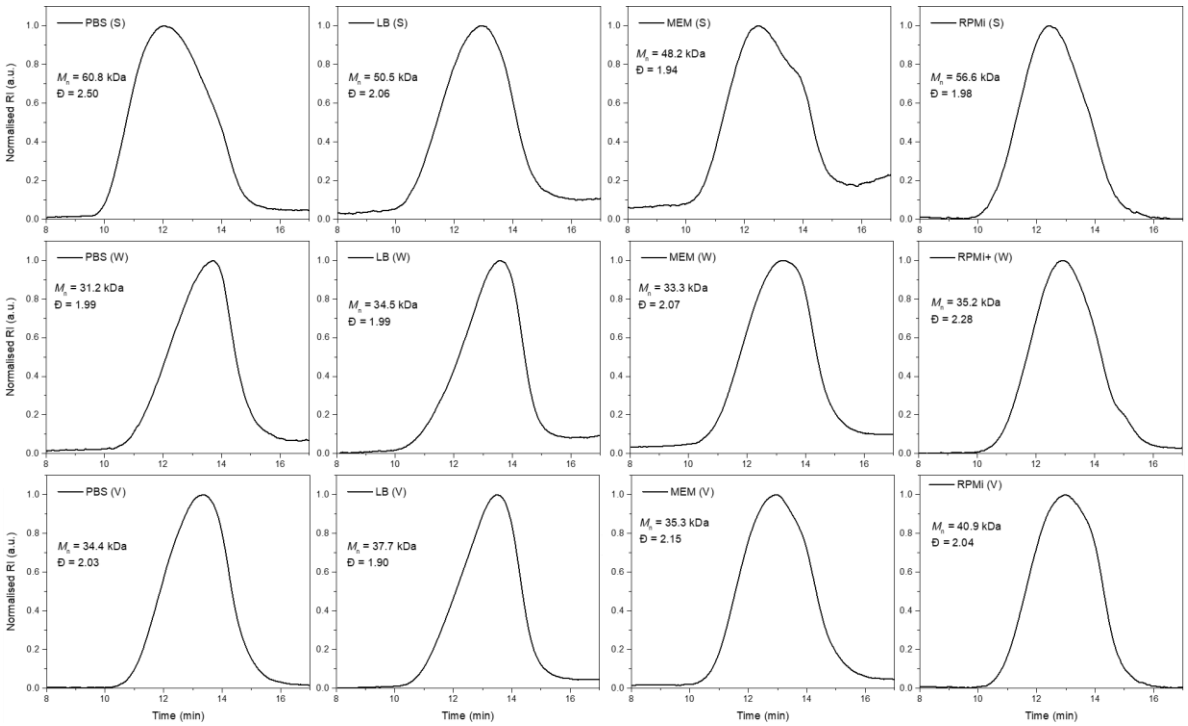

Figure S12. SEC (THF, 30 °C, PS standard) chromatogram of the purified mPEG-*b*-PHPMA copolymers from different morphologies (spheres: [HPMA] = 10 wt% and aimed DP = 150, worms: [HPMA] = 20 wt% and aimed DP = 150, vesicles: [HPMA] = 20 wt% and aimed DP = 300) synthesised by bioPISA in different media (PBS, LB, MEM and RPMi).

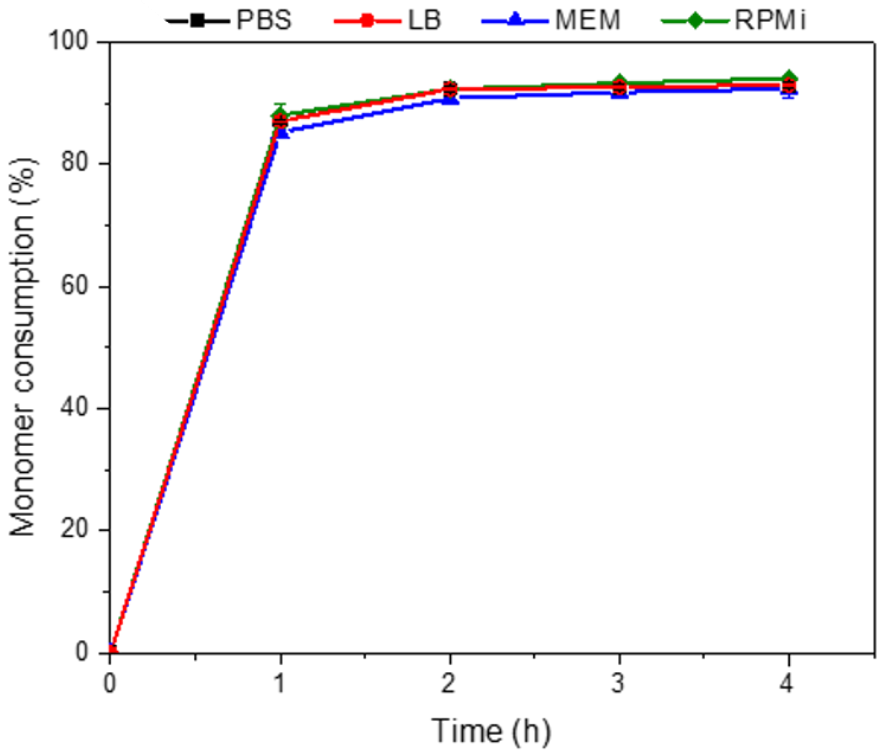

Figure S13. Monomer consumption over time ([HPMA] = 20 wt% and aimed DP = 150) in different media: PBS (black squares), LB broth (red circles), MEM (blue triangles) and RPMi-1640 (green diamonds). Error bars as mean ± SD, n = 3.

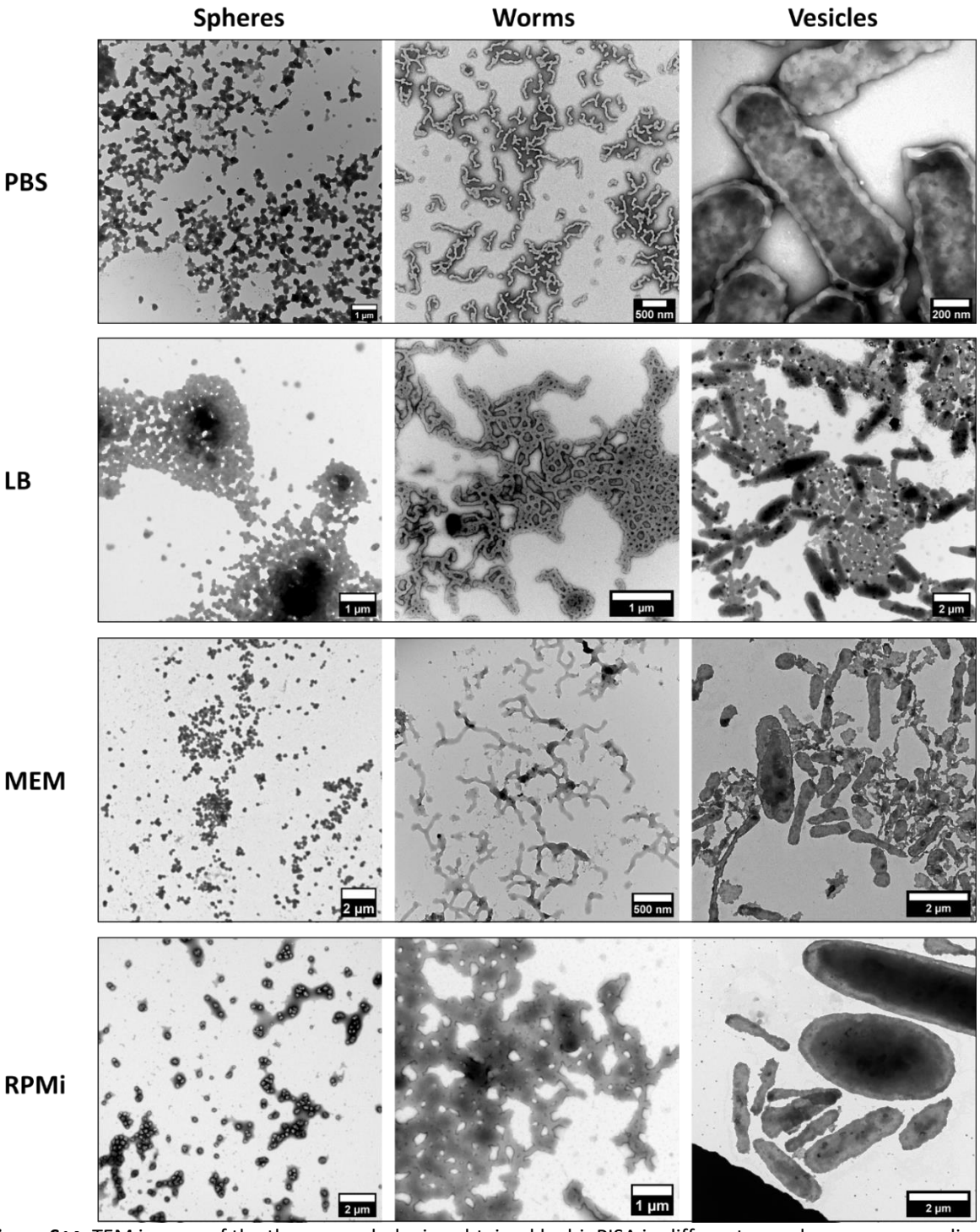

Figure S14. TEM images of the three morphologies obtained by bioPISA in different complex aqueous media (PBS, LB, MEM, RPMi) at [HPMA] = 10 wt% and aimed DP = 150 for the spheres, [HPMA] = 20 wt% and aimed DP = 150 for the worms and [HPMA] = 20 wt% and aimed DP = 300 for the vesicles.

BIOCOMPATIBILITY AND BACTERIAL ENCAPSULATION

To test the compatibility of bioPISA with living cells, bioPISA reactions were performed in the presence of bacteria. After bioPISA the bacteria were located both inside and outside of the self-assembled polymer structures. Although either the interactions of *Escherichia coli* with the polymer chains, or the extracellular environment altered the self-assembly process, resulting in filled microparticles (**Figure S15**), we could observe spatial association of the bacteria with the polymer and encapsulation of the bacteria within the polymer structures. Importantly, the live/dead assay for bacteria showed an acceptable viability (~70%) of these cells despite the use of an oxygen-free buffer that furthermore did not contain any nutrients and was rich in bromide ions, suggesting the biocompatibility of bioPISA (Figure S16).

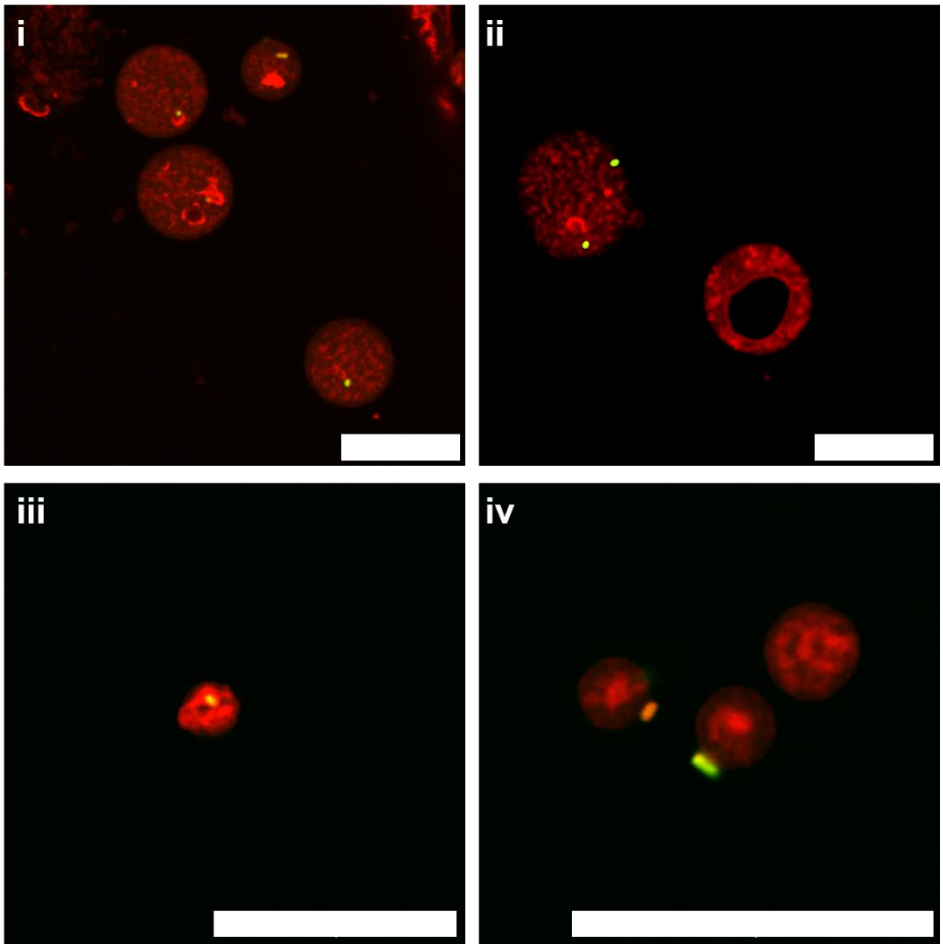

Figure S15. i-iv) Several CLSM micrographs of bioPISA-derived microparticles containing fluorescent *E. coli*. (Green: mClover expressed in *E. coli*, red: Cy5-$PEG_{3.5k}$-cholesterol). Scalebars: **20 µm.**

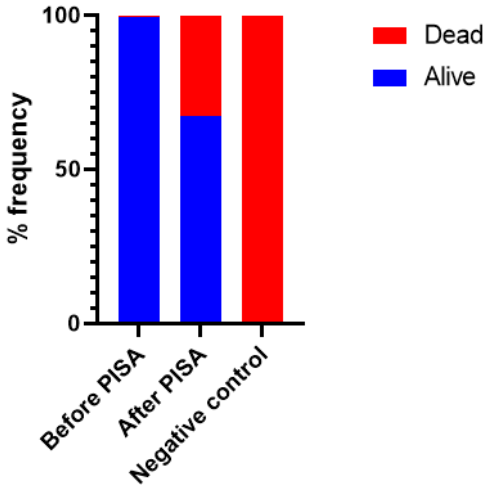

Figure S16. Live/dead assay of bacteria, showing their survival during bioPISA in PBS-Br. The negative control was provided by cells incubated at 95 °C for 10 minutes.

REACTION OVERVIEW

Table S2. Overview of the bioPISA reactions and copolymers characterisation

[HPMA] (wt%)	*Aimed HPMA DP*	*Solvent*	M_n (kDa)[a]	$Đ$[a]	*Monomer consumption (%)*[b]	*Morphology*[c]
5	150	PBS	-	-	17	-
5	200	PBS	-	-	44	-
5	250	PBS	-	-	39	-
5	300	PBS	-	-	44	-
5	350	PBS	-	-	56	-
5	400	PBS	-	-	53	-
10	150	PBS	-	-	13[d]	-
10	150	PBS	-	-	15[e]	-
10	-	PBS	-	-	12[f]	-
10	150	PBS	60.8	2.50	95	Spheres
10	150	LB	50.5	2.06	94	Spheres
10	150	MEM	48.2	1.94	88	Spheres
10	150	RPMi	56.6	1.98	92	Spheres
10	200	PBS	54.2	2.17	92	Mixed
10	250	PBS	45.2	1.99	95	Mixed
10	300	PBS	64.6	2.20	78	Spheres
10	350	PBS	51.9	2.58	60	Mixed
10	400	PBS	40.0	1.92	38	Mixed
15	150	PBS	28.5	1.99	96	Worms
15	200	PBS	34.8	2.12	92	Worms
15	250	PBS	37.7	1.78	87	Mixed
15	300	PBS	35.3	1.92	94	Mixed
15	350	PBS	35.5	1.69	86	Mixed
15	400	PBS	29.1	1.98	39	Mixed
20	150	PBS	31.2	1.99	93	Worms
20	150	LB	35.0	1.98	93	Worms
20	150	MEM	33.3	2.07	93	Worms

20	150	RPMi	35.0	2.09	95	Worms
20	200	PBS	28.5	1.96	94	Worms
20	250	PBS	30.2	1.96	91	Mixed
20	300	PBS	34.4	2.01	95	Vesicles
20	300	LB	34.7	1.91	90	Vesicles
20	300	MEM	35.3	2.15	90	Vesicles
20	300	RPMi	37.6	2.05	95	Vesicles
20	350	PBS	30.0	1.92	96	Vesicles
20	400	PBS	30.0	1.99	95	Vesicles
25	150	PBS	29.9	1.98	93	Worms
25	200	PBS	27.3	1.97	94	Mixed
25	250	PBS	33.4	1.99	94	Vesicles
25	300	PBS	29.9	1.90	95	Vesicles
25	350	PBS	29.5	1.89	95	Vesicles
25	400	PBS	31.4	1.96	95	Vesicles

[a] Determined by SEC (THF, 30 °C, PS standard). [b] Determined by ^{1}H NMR spectroscopy (DMSO-d_6). [c] Determined by dry-state TEM microscopy. [d] Control reaction without NaAsc. [e] Control reaction without Mb. [f] Control reaction without mPEG-Bib.

ENCAPSULATION AND MEMBRANE PERMEABILITY

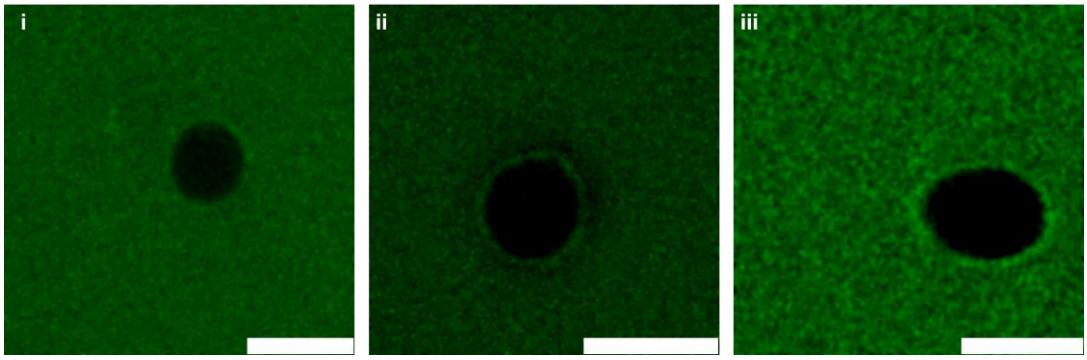

Figure S17. i-iii) Several CLSM micrographs of GUVs in a solution of FITC-Dextran 40 kDa. The vesicles are not fluorescent due to the impermeability of the membrane for the fluorescent dye (Green: FITC-Dextran 40 kDa). Scalebars: **10 µm.**

PURIFICATION OF GUVS VIA SIZE-EXCLUSION CHROMATOGRAPHY

Short PD 10 desalting columns have a claimed retention cut-off of 5000 Da. However, they were also previously reported to be able to separate low-concentration of proteins from vesicles.[14] To test whether they could be used for the separation of GUVs and cargo proteins, we recovered the first fraction (vesicles), washed it 1x with PBS, and then measured the Mb activity of the fractions before and after the washing steps, showing that the washed Mb-loaded GUVS had a similar activity than the original 1st fraction while the supernatant after washing had a much lower activity compared to the washed vesicles (**Figure S18**a). Thus, active protein of the 1st fraction resided in the vesicles and not in the surrounding solution. Similarly, the protein content in the vesicle-free supernatant was much lower than in the vesicles (**Figure S18**b). Finally, GUVs encapsulating ALP were washed during 4 cycles, and incubated with trypsin (0.5 mg mL^{-1}) for 1 hour. Both vesicles before and after washing retained their activity regardless of trypsinization, whereas the little activity detected in supernatants was annihilated with enzymatic digestion (**Figure S18**c), thus confirming the successful purification of free enzyme from the GUVs.

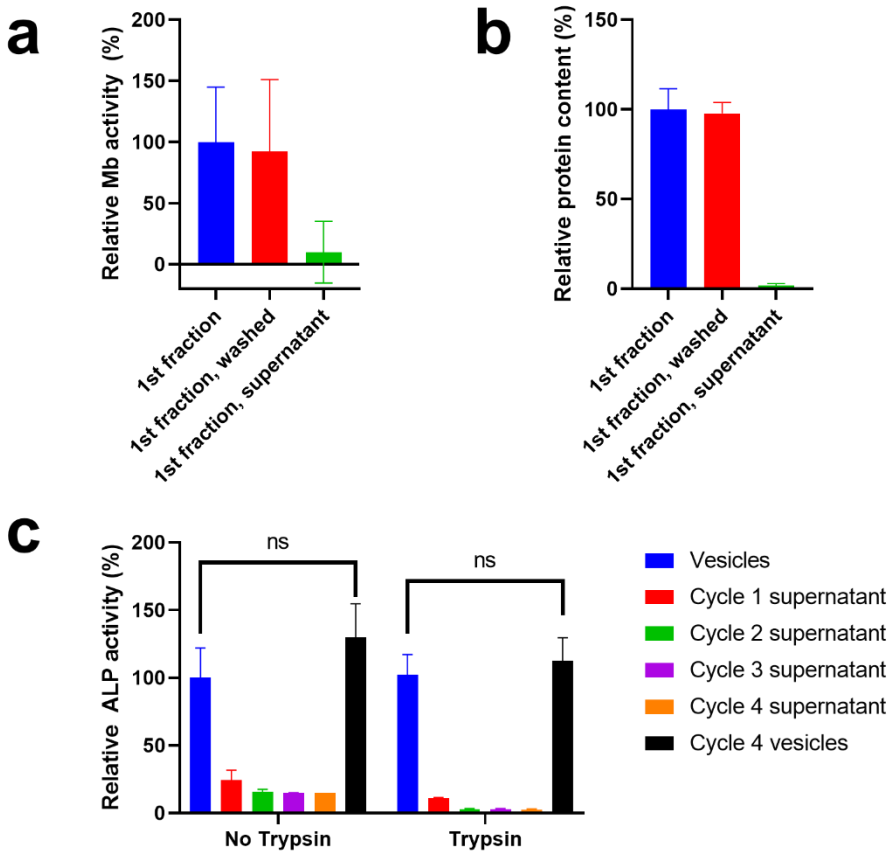

Figure S18. Purification of GUVs using PD 10 desalting columns. a) Relative Mb activity (oxidation of Ampex Red) from GUVs, GUVs after washing and resulting supernatant. b) Relative protein content from GUVs, GUVs after washing and resulting supernatant. c) Relative ALP activity (production of pNP from pNPP) of several fractions, with and without trypsin treatment. Mean ± SD, n=3.

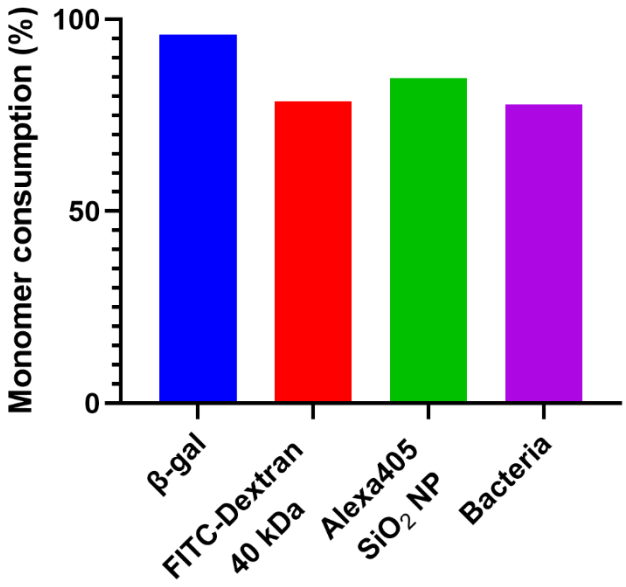

Figure S19. Monomer consumption during bioPISA in the presence of a selection of cargoes, showing the general tolerance of bioPISA for these bulky payloads.

ACTIN POLYMERIZATION

The resulting structures were similar to intracellular phase transitions driven by intrinsically disordered proteins, rather than previously seen filaments (**Figure S20**).[15] These structures could not be observed in absence of Mg^{2+}(**Figure S21**), nor with only the added cation, without actin (**Figure S22**), confirming that only the interplay between polymerized actin and polymer membrane yielded these unique structures.

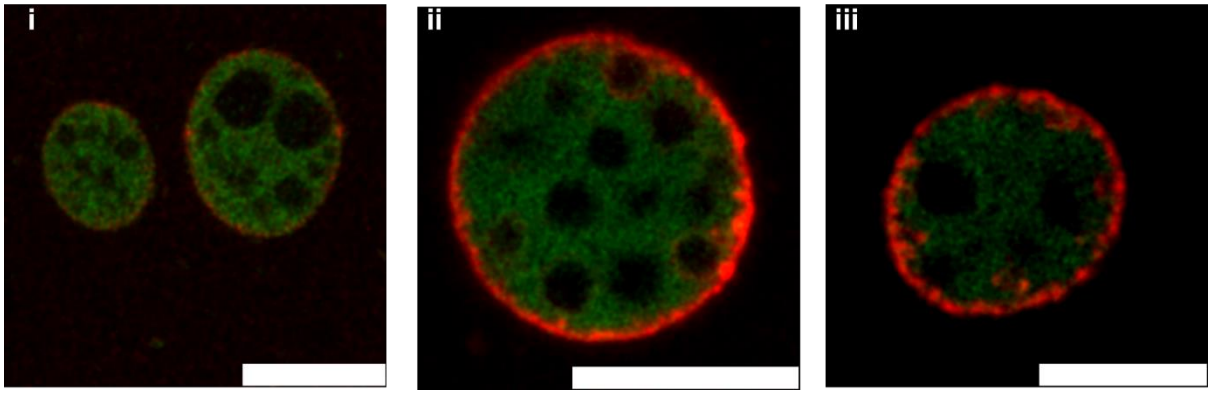

Figure S20. i-iii) Several CLSM micrographs of GUVs after the formation of actin condensates (actin/actin-Atto488/filamin: 1/0.25/0.01 weight ratio; green: actin-Atto488, red: Cy5-$PEG_{3.5k}$-cholesterol; the cholesterol dye could only label some of the inner vesicles)**The cholesterol dye could only label some of the inner vesicles. Scalebars: 10 µm.**

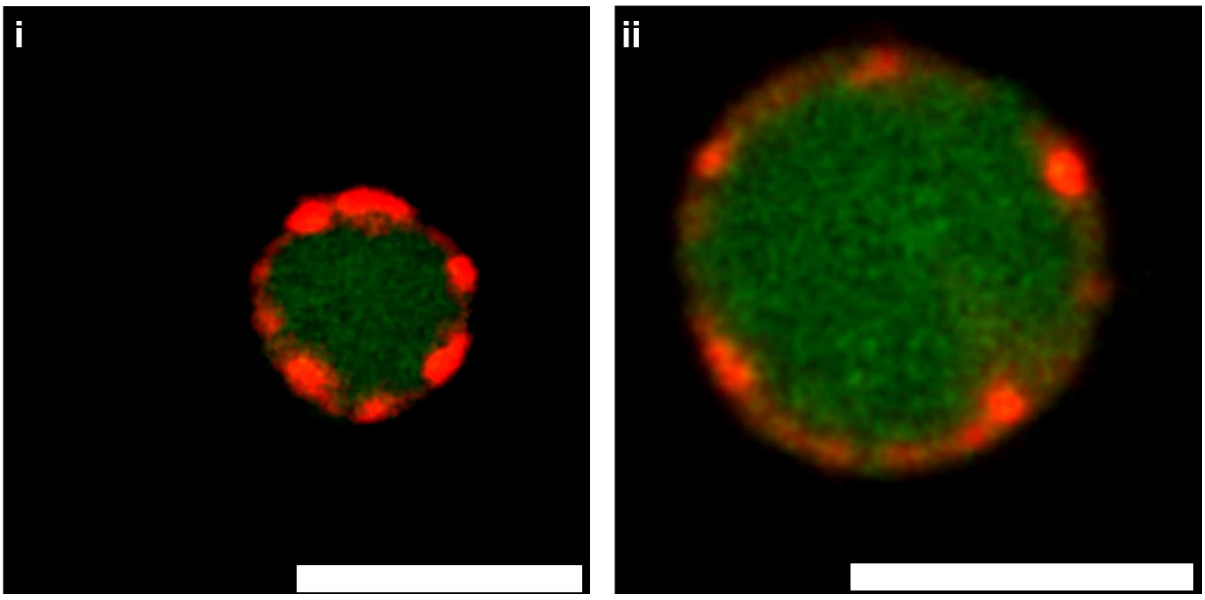

Figure S21. i-ii) Several CLSM micrographs of GUVs before the formation of actin condensates (actin/actin-Atto488/filamin: 1/0.25/0.01 weight ratio; green: actin-Atto488, red: Cy5-$PEG_{3.5k}$-cholesterol; the cholesterol dye could only label some of the inner vesicles)**The cholesterol dye could only label some of the inner vesicles. Scalebars: 5 µm.**

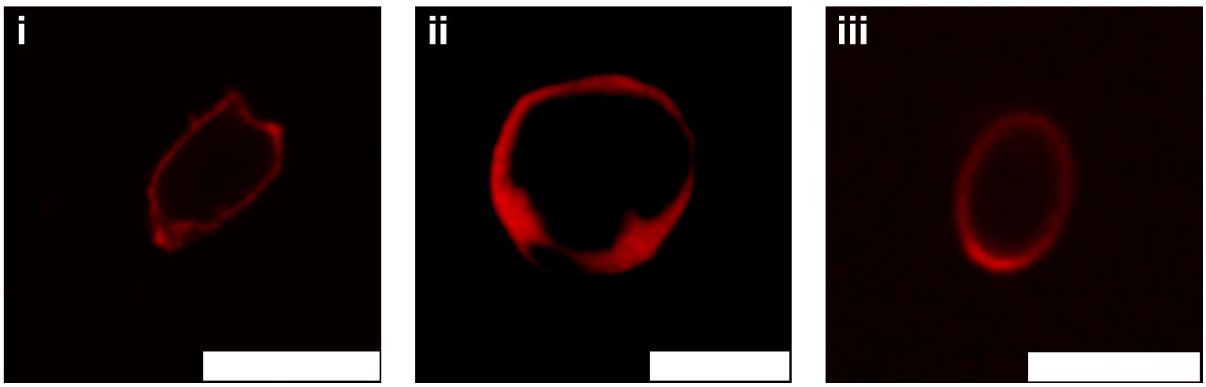

Figure S22. i-iii) Several CLSM micrographs of GUVs after addition of $MgCl_2$. Red: Cy5-PEG3.5k-cholesterol. The higher magnesium ion concentration appears to produce some deformations in the GUVs, but no subcompartment can be observed. Scalebars: 10 µm.

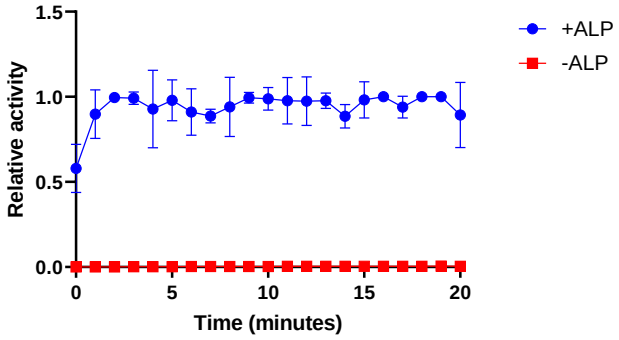

Figure S23. Activity of encapsulated ALP in bioPISA GUVs hydrolysing *p*-nitrophenyl phosphate (pNPP) to produce the phosphate-less coloured species pNP, showing that the enzyme is still active in the GUVs. All values displayed as mean ±SD, n=3 replicates for all experiments.

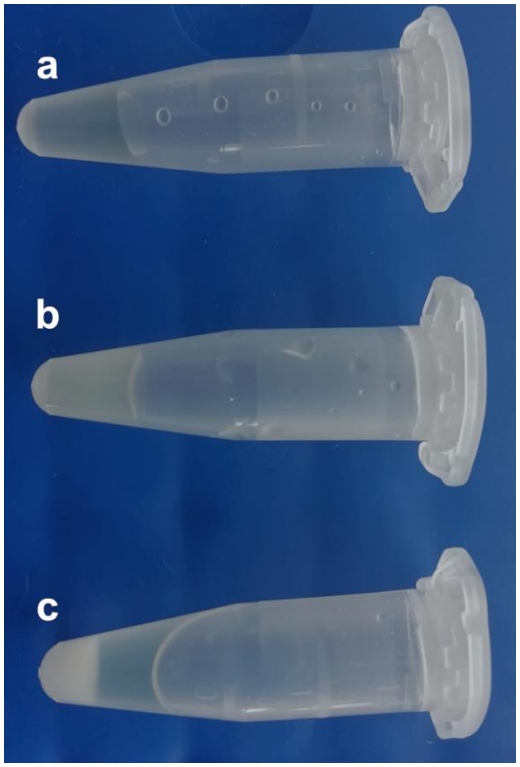

Figure S24. Co-precipitation of calcium phosphate and ALP in GUVs. a) CaGP, no GUVs. b) GUVs, no CaGP. c) GUVs + CaGP, leaving a clear supernatant in the last sample.

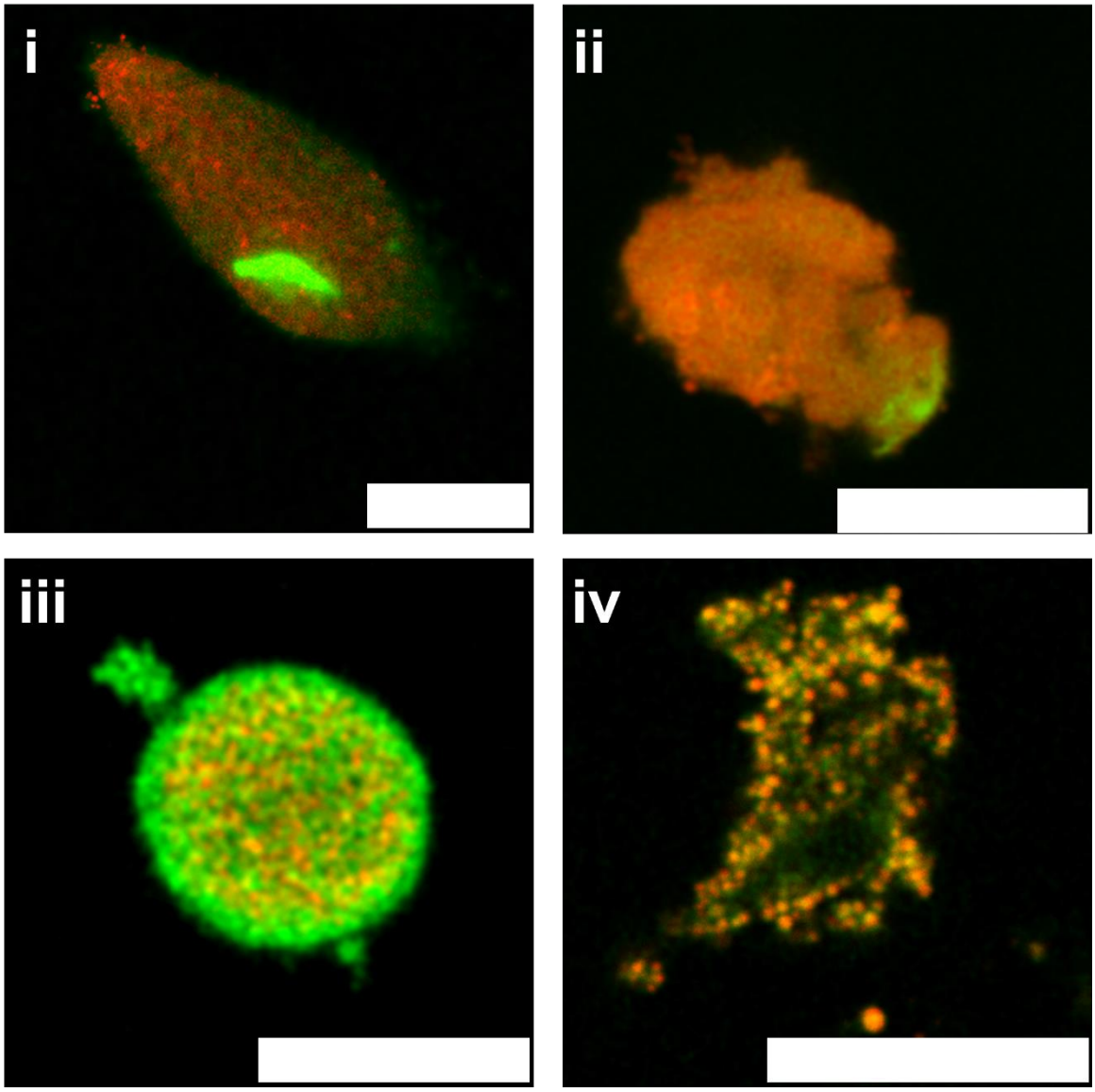

Figure S25. i – iv) Several CLSM micrographs of GUVs after the biomineralization of CaGP by ALP. Green: calcium phosphate-adsorbed fluorescein. Red: Cy5-PEG3.5k-cholesterol. Scalebars: 10 µm.

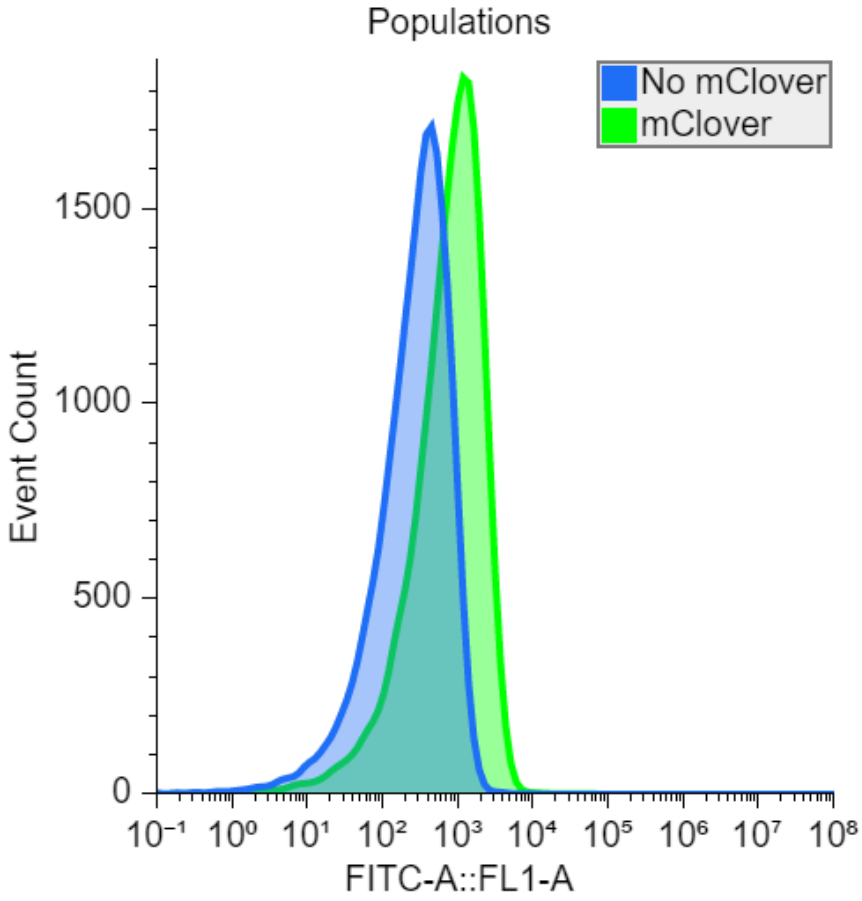

Figure S26. Flow cytometry fluorescence distributions for GUVs without and with plasmid, after the expression of mClover in the GUVs.

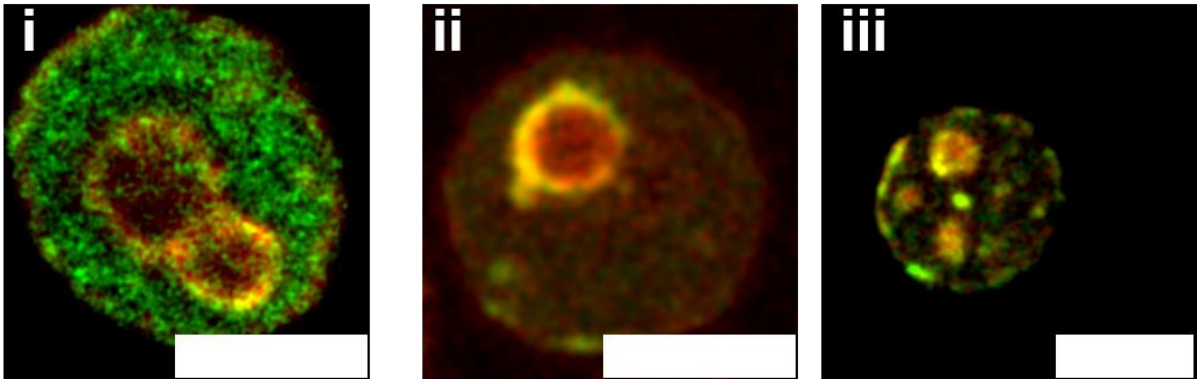

Figure S27. i – iii) CLSM micrographs of GUVs with expressed actin + phalloidin-Atto565 (green: phalloidin-Atto565, red: Cy5-$PEG_{3.5k}$-cholesterol**. Scalebars: 10 µm. Actin expression levels likely vary from GUV to GUV, and thus the morphologies it produces.**

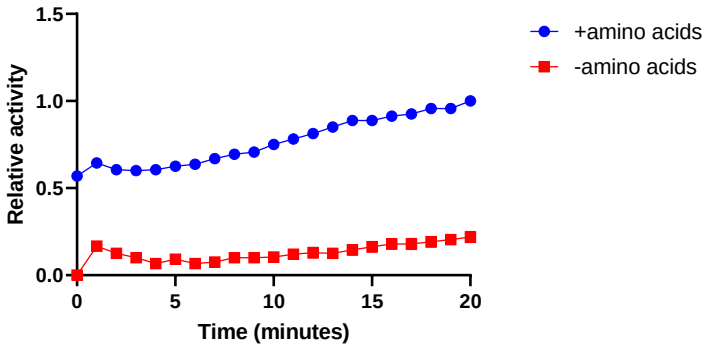

Figure S28. Activity of GUVs expressing ALP (decreased expression without supplemented amino acids) hydrolysing *p*-nitrophenyl phosphate (pNPP) to produce the phosphate-less coloured species pNP, plateauing earlier for GUVs + amino acids. All values displayed as mean ±SD (values too small to be displayed), n=3 replicates for all experiments.

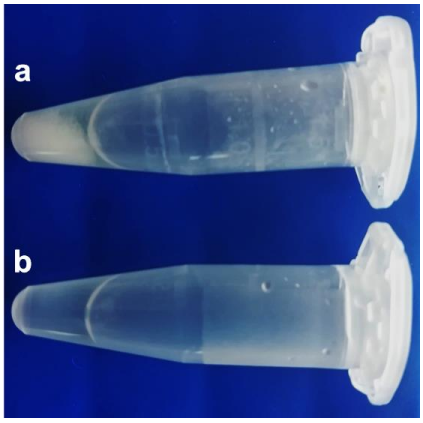

Figure S29. Co-precipitation of calcium phosphate and expressed ALP in GUVs. a) GUVs + expressed ALP + CaGP. b) GUVs + CaGP but no ALP expression.

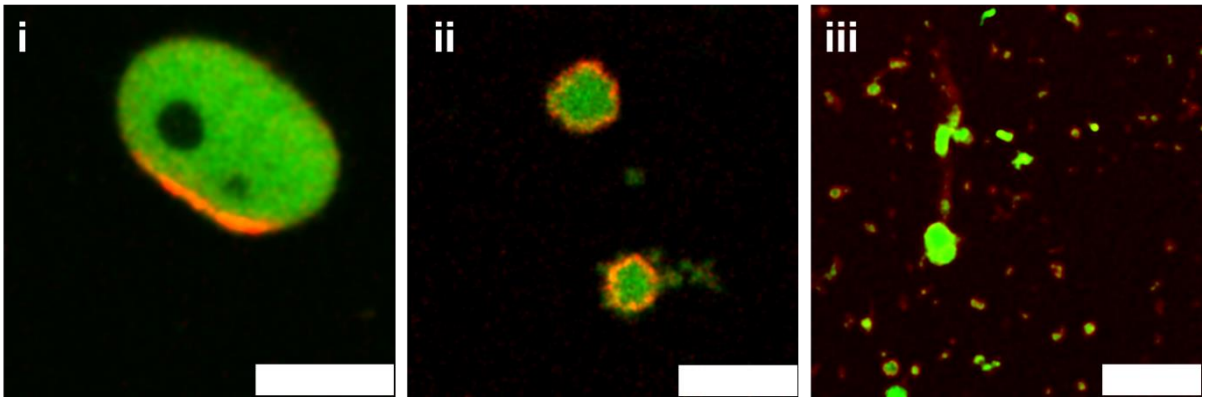

Figure S30. i-iii) Several CLSM micrographs of GUVs after the biomineralization of CaGP by expressed ALP. Green: calcium phosphate-adsorbed fluorescein. Red: Cy5-PEG3.5k-cholesterol. Scalebars: 10 µm.

1 Moreno-Echeverri, A. M. *et al.* Pitfalls in methods to study colocalization of nanoparticles in mouse macrophage lysosomes. *Journal of Nanobiotechnology* **20**, 464, doi:10.1186/s12951-022-01670-9 (2022).

2 Bajar, B. T. *et al.* Improving brightness and photostability of green and red fluorescent proteins for live cell imaging and FRET reporting. *Sci Rep* **6**, 20889, doi:10.1038/srep20889 (2016).

3 Rowan, S. & Cepko, C. L. A POU factor binding site upstream of the Chx10 homeobox gene is required for Chx10 expression in subsets of retinal progenitor cells and bipolar cells. *Developmental biology* **281**, 240-255, doi:10.1016/j.ydbio.2005.02.023 (2005).

4 de Graaf, A. J. *et al.* ATRP, subsequent azide substitution and 'click' chemistry: three reactions using one catalyst in one pot. *Chemical Communications* **47**, 6972-6974, doi:10.1039/C1CC12224J (2011).

5 Belluati, A., Harley, I., Lieberwirth, I. & Bruns, N. *An outer membrane-inspired polymer coating protects and endows E. coli with novel functionalities.* (2022).

6 Gill, S. C. & von Hippel, P. H. Calculation of protein extinction coefficients from amino acid sequence data. *Analytical Biochemistry* **182**, 319-326, doi:https://doi.org/10.1016/0003-2697(89)90602-7 (1989).

7 Khor, S. Y., Truong, N. P., Quinn, J. F., Whittaker, M. R. & Davis, T. P. Polymerization-Induced Self-Assembly: The Effect of End Group and Initiator Concentration on Morphology of Nanoparticles Prepared via RAFT Aqueous Emulsion Polymerization. *ACS Macro Letters* **6**, 1013-1019, doi:10.1021/acsmacrolett.7b00583 (2017).

8 Teodorescu, M. & Matyjaszewski, K. Atom Transfer Radical Polymerization of (Meth)acrylamides. *Macromolecules* **32**, 4826-4831, doi:10.1021/ma990175x (1999).

9 D'hooge, D. R. *et al.* Assessment of end-group functionality in atom transfer radical polymerization of N-isopropylacrylamide. *European Polymer Journal* **49**, 2344-2355, doi:https://doi.org/10.1016/j.eurpolymj.2013.05.019 (2013).

10 Ribelli, T. G., Lorandi, F., Fantin, M. & Matyjaszewski, K. Atom Transfer Radical Polymerization: Billion Times More Active Catalysts and New Initiation Systems. **40**, 1800616, doi:https://doi.org/10.1002/marc.201800616 (2019).

11 Connell, L. S., Jones, J. R. & Weaver, J. V. M. Transesterification of functional methacrylate monomers during alcoholic copper-catalyzed atom transfer radical polymerization: formation of compositional and architectural side products. *Polymer Chemistry* **3**, 2735-2738, doi:10.1039/C2PY20280H (2012).

12 Save, M., Weaver, J. V. M., Armes, S. P. & McKenna, P. Atom Transfer Radical Polymerization of Hydroxy-Functional Methacrylates at Ambient Temperature: Comparison of Glycerol Monomethacrylate with 2-Hydroxypropyl Methacrylate. *Macromolecules* **35**, 1152-1159, doi:10.1021/ma011541r (2002).

13 Wang, G. *et al.* Polymerization-Induced Self-Assembly (PISA) Using ICAR ATRP at Low Catalyst Concentration. *Macromolecules* **49**, 8605-8615, doi:10.1021/acs.macromol.6b01966 (2016).

14 Shetty, S. C. *et al.* Directed Signaling Cascades in Monodisperse Artificial Eukaryotic Cells. *ACS Nano* **15**, 15656-15666, doi:10.1021/acsnano.1c04219 (2021).

15 Shin, Y. *et al.* Spatiotemporal Control of Intracellular Phase Transitions Using Light-Activated optoDroplets. *Cell* **168**, 159-171.e114, doi:10.1016/j.cell.2016.11.054 (2017).